Proc. of the 5th WSEAS/IASME Int. Conf. on Electric Power Systems, High Voltages, Electric Machines, Tenerife, Spain, December 16-18, 2005 (pp256-261)

Performance Assessment Of Fuzzy Logic Based Power System Stabilizer

E. A. FEILAT* A. M. JAROSHI
Hijjawi Faculty for Engineering Technology
Yarmouk University
Irbid 21163, Jordan

S. M. RADAIDEH
Electrical Engineering Department
Jordan University of Science and Technology
Irbid, Jordan

Abstract:- This paper investigates the performance of fuzzy logic based power system stabilizer in damping the local modal oscillations of an interconnected power system. A comparative study between Mamdani and Sugeno fuzzy logic designs on one hand and conventional power system stabilizers on the other hand is presented. The results obtained by computer simulation show the superiority of fuzzy logic controllers over the conventional designs. The test results also show the effectiveness of Mamdani design relative to Sugeno design in damping the electromechanical mode of oscillation.

Key-Words:- Power System Stability, Power System Stabilizer, Fuzzy Logic, Adaptive Control, Simulation

1 Introduction

Interconnected power systems usually experience low-frequency oscillations following gradual load changes due to insufficient damping. These modes of oscillations occur particularly between one machine and the rest of a power system with longitudinal or weak tie lines or between interconnected machines. They result from the existence of one or several poorly damped or even undamped modes of oscillations in the range of 0.7-2 Hz for local modes and 0.1-0.7 Hz for inter-area modes [1-3]. The stability of these oscillations is of vital concern and essential for power system planning, operation, and control.

It was also reported that one of the reasons for the presence of these oscillation is the application of high gain AVR-exciter system. High gain exciter of AVR increases the synchronizing torque but reducing the damping torques [4].

To compensate the unwanted effect of the voltage regulator and enhance the overall power system stability, by damping the low-frequency modes of oscillations over wide range of operating conditions, additional signal is introduced in the feedback loop of the voltage regulator. This is achieved by injecting a stabilizing signal or some times signals in parallel into the excitation system voltage reference-summing junction. The additional signals are mostly speed deviation, accelerating power, or frequency [5]. The devices set up to provide the supplementary stabilizing signal in the excitation system through properly chosen transfer function, have been called "power system stabilizer" (PSS).

Conventional designs of PSS including phase lead-lag compensators or PID controllers were typically designed based on linear control theory using the concept of phase compensation [3] or pole assignment techniques [6-9]. The parameters are determined based on a linearized model of the power system around a nominal operating point where they can provide optimum damping performance of low-frequency oscillations at a particular operating point. Moreover, to achieve robust performance over a wide range of operating conditions by tuning the PSS parameters several adaptive control techniques were developed [10,11].

Recently, artificial intelligence techniques based on neural networks (NN) [12-14], genetic algorithms (GI) [15], and fuzzy logic (FL) [16-21] have been proposed. Fuzzy logic-based PSS (FLPSS) has shown promising results in enhancing the damping of oscillations, in particular when adaptive FLPSS were used. [18-21]

In this paper, a comparative study between the performance of Mamdani and Sugeno fuzzy logic-based PSS's is presented. The effect of membership functions and fuzzy aggregation types of Mamdani FL model is examined. The performance of the FLPSS is compared with a conventional lead-lag PSS (CPSS). The simulation study was conducted using MATLAB fuzzy logic toolbox [22].

2 Description of the Study System

To study the performance of FLPSS in damping the local mode oscillations associated with a single

generator or plant, the single machine infinite bus system (SMIBS), as shown in Fig. 1, is used. The generator is represented by a third-order machine model and is equipped with automatic voltage regulator (AVR) and PSS [2].

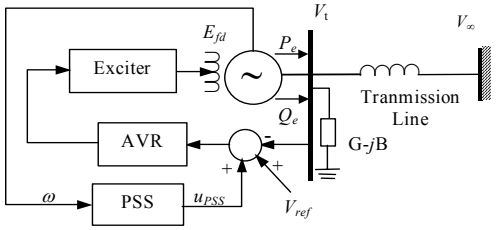

Fig.1: Single Machine Infinite Bus System

The design of conventional PSS's requires linearization of the power system at a particular operating point to obtain the state-space model

$$\dot{\boldsymbol{x}} = \boldsymbol{Ax} + \boldsymbol{Bu}$$
$$\boldsymbol{y} = \boldsymbol{Cx} + \boldsymbol{Du} \qquad (1)$$

where $\boldsymbol{x} = \left[\Delta\omega \quad \Delta\delta \quad \Delta e'_q \quad \Delta E_{fd} \quad \Delta x_5 \quad \Delta x_6 \quad \Delta u_{PSS}\right]^T$, $\boldsymbol{y} = \left[\Delta\omega\right]$ and $\boldsymbol{u} = \left[\Delta T_m \quad \Delta V_{ref}\right]^T$; Δ denotes the perturbation of the states, inputs and output from their operating values. The linearized model of the SMIBS can be derived with the aid of the well-known Phillips-Heffron block diagram [3,4]; relating the pertinent variables such as electrical torque, speed, rotor angle, terminal voltage, field voltage and internal voltage as shown in Fig.2. The parameters of the linearized model K_1-K_6 are function of the operating conditions. Analysis and calculations of the parameters of the SMIBS are illustrated in details in [3,4]. The small signal stability response in terms of the change in the rotor speed $\Delta\omega$ following a small change in the mechanical torque ΔT_m or the reference voltage ΔV_{ref} can be simulated with the aid of the block diagram of the SMIBS or the state-space model. Dynamic data of the generator and excitation system under study, and the matrices of the state-space model, constructed from typical machine parameters at specific operating point, are given in [3].

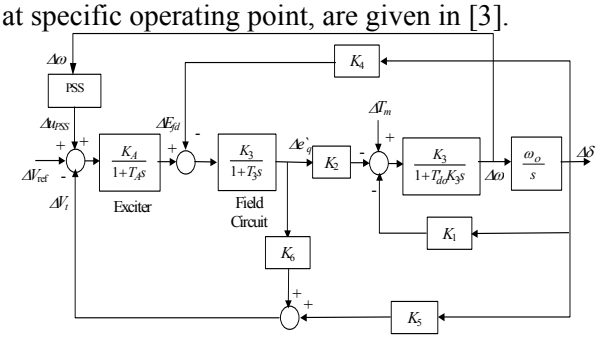

Fig.2: Heffron-Phillips Block diagram of SMIBS

3 Analysis of Local Mode Oscillations

When the power system experiences a small disturbance as a result of small changes of loads, the system will be driven to an initial state $\boldsymbol{x}(t_o) = \boldsymbol{x_o}$ at time $t_o = 0$. Then, if the input is removed at $t = t_o$, the system responds according to the state equations

$$\dot{\boldsymbol{x}} = \boldsymbol{Ax}$$
$$\boldsymbol{y} = \boldsymbol{Cx} \qquad (2)$$

The state equations of the linearized model given in (2) can be used to determine the eigenvalues λ_i of the system matrix $\boldsymbol{A}$, where $\lambda_i = \sigma_i \pm j\omega_i$ are the distinct eigenvalues with a corresponding set of right and left eigenvectors U_i and V_i, respectively; σ_i is the damping factor and ω_i is the damped angular frequency. The right and left eigenvectors are orthogonal, and are usually scaled to be orthonormal. The state equations of (2) can be expressed in terms of modal variables by using the modal transformation $\boldsymbol{x} = \boldsymbol{Uz}$, which leads to

$$\dot{\boldsymbol{z}} = \boldsymbol{V}_i \boldsymbol{A} \boldsymbol{U}_i \boldsymbol{z} = \boldsymbol{\Lambda z} \qquad (3)$$

where $\boldsymbol{\Lambda}$=diag(λ_i). Following a small disturbance, the dynamic response of the system states can be described as a linear summation of various modes of oscillations [1]

$$\boldsymbol{x}(t) = \sum_{i=1}^{n} \boldsymbol{U}_i \left(\boldsymbol{V}_i \boldsymbol{x}_o\right) e^{\lambda_i t} \qquad (4)$$

The number of the characteristic modes $e^{\lambda_i t}$ equals to the number of states of the linearized power system model. Real eigenvalues indicate modes, which are aperiodic. Complex eigenvalues indicate oscillatory modes. For a complex eigenvalue $\lambda_i = \sigma_i \pm j\omega_i$, the amplitude of the mode varies with as $e^{\sigma_i t}$ and frequency of the oscillation, $f = \omega/2\pi$.

For a single output, the system response $y(t)$ can be computed as

$$y(t) = \sum_{i=1}^{n} B_i e^{\lambda_i t} = \sum_{i=1}^{n} A_i e^{\sigma_i t} \cos(2\pi f_i t + \phi_i) \qquad (5)$$

where A_i, σ_i, f_i,and ϕ_i are the i^{th} mode amplitude, damping factor, frequency, and phase angle, respectively, and n is the number of modes.

Next, an analysis is performed to find the specific electromechanical mode that provides the largest contribution to the low-frequency oscillation. In modal analysis, the electromechanical mode is identified by analyzing the right and left eigenvectors in conjunction with the participation factors [1]. The participation factors provide a measure of association between the state variables and the oscillatory modes.

4 Power System Stabilizer Design

4.1 Conventional PSS Design

PSS typically is designed based on linear control theory using the concept of phase compensation [4]. The parameters are determined so that they can provide optimum damping performance of low-frequency oscillations. Phase compensation is accomplished by adjusting the PSS parameters to provide a appropriate phase lead to compensate for the phase lags through the generator, AVR and excitation system over a wide frequency range (0.1-2.0 Hz) of low frequency oscillations such that the PSS provides torque changes $\Delta T_e(t)$ in phase with speed changes $\Delta\omega(t)$. Tuning should be performed when system configuration and operating conditions result in the least damping [3].

In this paper, a phase lead-lag CPSS has been used for performance comparison with FLPSS. The transfer function of the CPSS comprises a gain block K_c, a washout filter and two-stage lead-lag blocks. The input signal is the rotor speed deviation $\Delta\omega$, and the output is the stabilizing signal ΔU_{PSS}. The block diagram of the CPSS is shown in Fig. 3. In this study, T_w T_2, and T_4 were set at T_w= 5s, T_2= T_4= 0.1s, and T_1=T_3. The technique for calculating K_c and T_1 using phase compensation method is presented in [3].

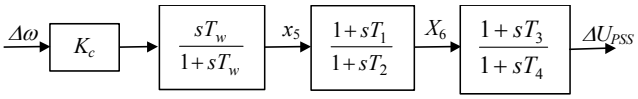

Fig.3: Phase Lead-Lag PSS

4.2 Fuzzy Logic PSS Design

The design of FLPSS using the two famous fuzzy Mamdani and Sugeno models is discussed. The input signals to the FLPSS are selected as generator speed deviation $\Delta\omega$ and generator speed deviation change $\Delta\dot{\omega}$, while the output signal is the stabilizing signal U_{PSS}, which is fed into the reference voltage summing point. The input and output variables are classified into subsets of linguistic variables. Based on trail and error, seven linguistic variables for each input and output variable such as large negative (LN), medium negative (MN), small negative (SN), zero (Z), small positive (SP), medium positive (MP), and large positive (LP) were found good enough. These classifications get 49 Mamdani rules as given in Table 1. Too many rules will result in wasting computer memory and computing time, and too few rules will not give the appropriate control effort.

4.2.1 Mamdani FLC Design

In Mamdani FLC design, fuzzification is applied by converting the crisp values of the input variables into their associated fuzzy sets using either triangular or Gaussian membership functions as shown in Fig. 4. Each crisp input has seven values when it is fired with these membership functions.

Table 1: Rule Base Table of Mamdani FLC

Input ($\Delta\omega$)	Input ($\Delta\dot{\omega}$)						
	LN	MN	SN	Z	SP	MP	LP
	Output (U_{PSS})						
LN	LN	LN	LN	LN	MN	SP	Z
MN	LN	MN	MN	MN	SN	Z	SP
SN	LN	MN	SN	SN	Z	SP	MP
Z	LN	MN	SN	Z	SP	MP	LP
SP	MN	SN	Z	SP	SP	MP	LP
MP	SN	Z	SP	MP	MP	LP	LP
LP	Z	SP	MP	LP	LP	LP	LP

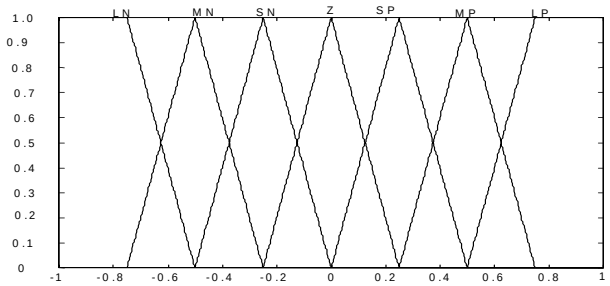

Fig. 4-a: Triangular Type Membership Functions

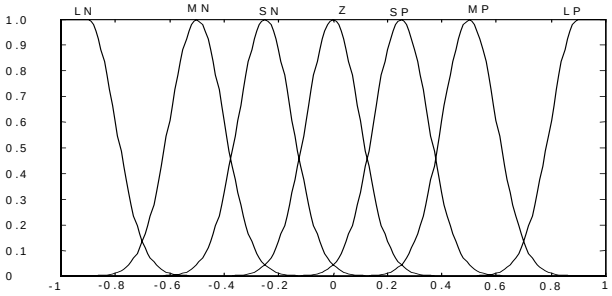

Fig. 4-b: Gaussian Type Membership Functions

Next, the fuzzy output of the FLC is defuzzified by converting it into a single value using the center of gravity

$$U^*_{PSS} = \frac{\sum_{i=1}^{n} \mu(U_{PSS\,i}) * U_{PSS\,i}}{\sum_{i=1}^{n} \mu(U_{PSS\,i})} \qquad (6)$$

where n is the number of discrete values (U_{PSS_i}) in the universe of discourse and μ is the membership grade.

The effect of the triangular and Gaussian membership functions on the performance of the

FLC with the same fuzzy sets and universe of discourse, and the effect of aggregation types (max-min-max, max-pro-max, and max-pro-sum) will be investigated.

4.2.2 Sugeno Zero-Order FLC Design

Sugeno zero-order model is considered as a special case of Mamdani model. In this regard, the output is considered as a singleton. Instead of considering the output control signal as a set of numbers, Sugeno method proposes a specific number as the output control signal U_{PSS} as given in Table 2.

Table 2: Rule Base Table of zero-order Sugeno FLC

Input ($\Delta\omega$)	Input ($\Delta\dot{\omega}$)						
	LN	MN	SN	Z	SP	MP	LP
	Output (U_{PSS})						
LN	-1.0	-1.0	-1.0	-1.0	-0.66	0.33	0.00
MN	-1.0	-0.66	-0.66	-0.66	-0.33	0.00	0.33
SN	-1.0	-0.66	-0.33	-0.33	0.00	0.33	0.66
Z	-1.0	-0.66	-0.33	0.00	0.33	0.66	1.0
SP	-0.66	-0.33	0.00	0.33	0.33	0.66	1.0
MP	-0.33	0.00	0.33	0.66	0.66	1.0	1.0
LP	0.00	0.33	0.66	1.0	1.0	1.0	1.0

5 Simulation Results

The effect of the fuzzy model on the performance of the FLPSS is investigated. Two types of fuzzy models were investigated, namely Mamdani and Sugeno zero-order models.

5.1 Performance of Mamdani FLPSS

The effect of Mamdani membership function type on the performance of the FLPSS is examined using the block schematic of the SMIB-FLPSS with triangular and Gaussian as shown in Fig.5. The results are depicted in Fig. 6. It can be seen that triangular Membership function gives better damping characteristics than Gaussian membership function. This is because it fires faster in triangular type than in the Gaussian type membership function.

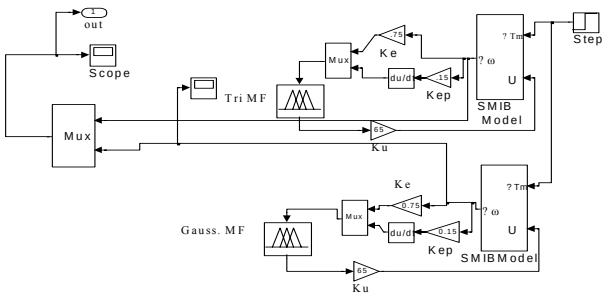

Fig. 5: SMIB-Mamdani FLPSS Block Schematic

The effect of implication & aggregation types on the performance of Mamdani FLPSS was also assessed. Figure 7 shows that the max-pro-sum performs well in comparison with the other types of aggregation. Figure 7 also indicates that max-min-max and max-pro-max aggregations exhibit identical performance over wide range of operating conditions.

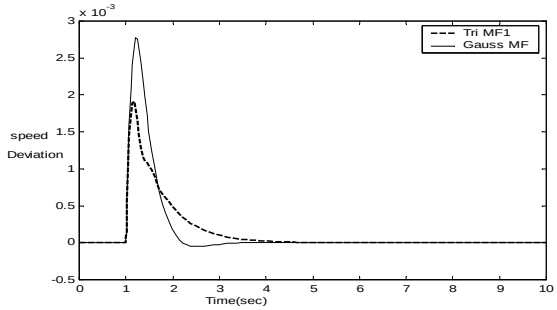

Fig. 6: Effect of Membership Function. P=1.0 pu, Q=0.015 pu

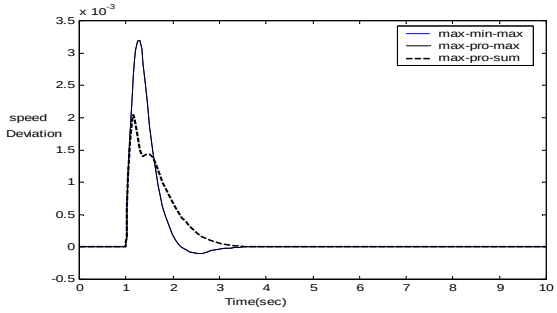

Fig. 7: Effect of Implication and Aggregation Types. P=1.0 pu, Q= 0.015 pu

Following the proper choice of membership functions and aggregation type of Mamdani FLPSS, a comparison between the FLPSS and Lead-Lag CPSS is depicted in Fig. 8. The parameters of the CPSS were computed so that near optimum performance at the particular operating point is satisfied. It can be seen that FLPSS using triangular membership function and max-min-sum perform better than the CPSS.

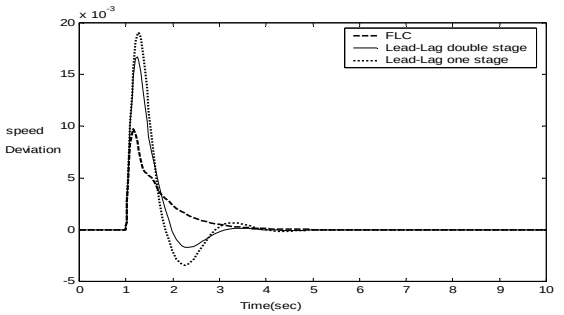

Fig.8: Performance Comparison Between Mamdani FLPSS and CPSS. P=1.0 pu, Q=0.015 pu

5.2 Performance of Sugeno FLPSS

Comparison between Sugeno zero-order FLPSS and Mamdani FLPSS using the schematic of Fig. 9 is demonstrated in Fig. 10. It can be seen that Sugeno FLPSS gives better damping characteristics than Mamdani FLPSS with Gaussian Membership function. However, Fig. 10 shows that the performance of Mamdani FLPSS with triangular membership function is more excellent than the performance of either Sugeno FLPSS or Mamdani FLPSS with Gaussian membership function.

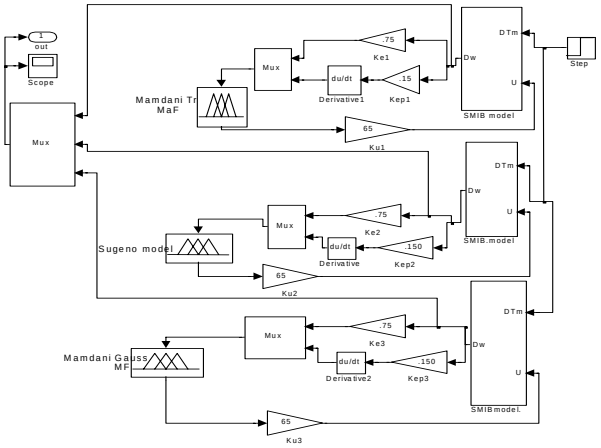

Fig. 9: SMIB-Sugeno-Mamdani FLPSS Block Schematic

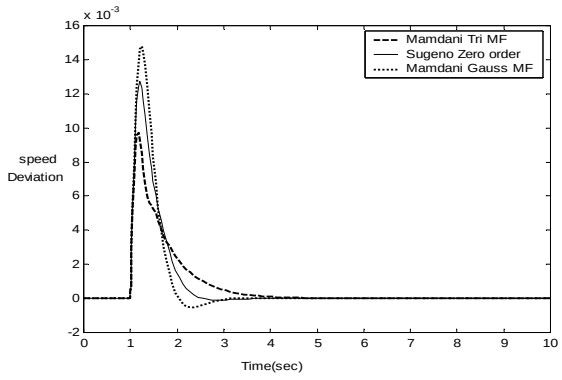

Fig.10: Performance Comparison Between Sugeno and Mamdani FLPSS's. P=1.0 pu, Q=0.015 pu

6 Conclusion

In this paper, a comparative study between the effectiveness of Mamdani and Sugeno fuzzy logic-based PSS's was investigated. The effect of membership functions and fuzzy aggregation types of Mamdani FL model was examined. The performance of the FLPSS is compared with a lead-lag CPSS. The simulation results show the effectiveness of FLPSS in damping the low-frequency modes of oscillation of interconnected power system as compared with a well designed lead-lag CPSS. The results also indicate the Mamdani FLPSS with triangular membership function give the best dynamic performance and excels the other FLC designs presented in this study.

References:

[1] P. Kundur, *Power System Stability and Control*, McGraw-Hill, 1994.

[2] P. Anderson and A. Fouad, *Power System Control and Stability.* Iowa State University Presses, 1997.

[3] Y. N. Yu, *Electric Power System Dynamics*, Academic Press, NY, 1983.

[4] F. P. DeMello and C. Concordia, Concepts of synchronous machine stability as affected by excitation control, *IEEE Trans*. *PAS,* Vol.88, No.5, 1969, pp. 316-329.

[5] R. Larsen and D. Swann, Applying power system stabilizers. Parts I-III, *IEEE Trans. PAS*, Vol.100, No.6, 1981, pp. 3017-3046.

[6] P. Kundur, M. Klein, and G. Rogers, Application of power system stabilizers for enhancement of overall system stability, *IEEE Trans. PWRS*, Vol.4, No.2, 1989, pp. 614-626.

[7] G. Chen, *Y.* Qin, G. Xu, and O. Malik, Optimization technique for the design of a linear optimal power system stabilizer, *IEEE Trans. EC*, Vol.7, No.3, 1992, pp. 453-459.

[8] J. Chow and J. Sanchez, Pole-placement designs of power system stabilizers. *IEEE Trans. PWRS*, Vol.4, No.1, 1989, pp. 271-277.

[9] M. El-Sherbiny, M. Hassan, G. El-Saady, and A. Yousef, Optimal pole shifting for power system stabilization. *Electric Power System Research.* Vol.66, 2003, pp. 253-258.

[10] A. Ghosh, G. Ledwich, O. Malik, and G. Hope, Power system stabilizer based on adaptive control techniques, *IEEE Trans. PAS*, Vol.103, No.8, 1984, pp. 1983-1989.

[11] S. Cheng, Y. Chow, O. Malik, and G. Hope, An adaptive synchronous machine stabilizer, *IEEE Trans. PAS*, Vol.1, No.3, 1986, pp. 101-109.

[12] Y. Y. Hsu and C. L. Chen, Tuning of power system stabilizers using an artificial neural network, *IEEE Trans. EC*, Vol.64, 1991, pp. 612-619.

[13] R. Segal, M. L. Kotari, and S. Madnani, Radial basis function network adaptive power system stabilizer, *IEEE Trans. PWRS*, Vol.15, No.2, 2000, pp. 722-727.

[14] Y. Zhang, G.P. Chen, O.P. Malik, and G.S. Hope, An artificial neural network based adaptive power system stabilizer, *IEEE Trans. EC*, Vol.8, No.1, 1993, pp. 71-77.

[15] J. Wen, S. Cheng, and O. P. Malik, A synchronous generator fuzzy excitation controller optimally designed with a genetic algorithm, *IEEE Trans. PWRS*, Vol.13, No.3, 1998, pp. 884-889.

[16] M. A. Hassan, O. P. Malik, and G. S. Hope, A fuzzy logic based stabilizer for a synchronous machine, *IEEE Trans. EC*, Vol. 6, No.3, 1991, pp. 407-413.

[17] H. Toliyat, J. Sadeh, and R. Ghazi, Design of augmented fuzzy logic power system stabilizers to enhance power systems stability, *IEEE Trans. EC*, Vol.11, No.1, 1996, pp. 97-103.

[18] P. Hoang and K. Tomsovic, Design and analysis of an adaptive fuzzy power system stabilizer, *IEEE Trans. EC*, Vol.11, No.2, 1996, pp. 455-461.

[19] T. Lie, and A. Sharaf, An adaptive fuzzy logic power system stabilizer. *Electric Power System Research.* Vol. 38, 1996, pp. 75-81.

[20] R. You, H. Eghbali, and M. Nehrir, An online adaptive neuro-fuzzy power system stabilizer for multi-machine systems, *IEEE Trans. PWRS*, Vol.18, No.1, 2003, pp. 128-135.

[21] M. Abido and Y. Abdel-Magid, Fuzzy basis function network based power system stabilizer for generator excitation control. *Electric Power System Research*, Vol.49, 1999, pp. 11-19.

[22] *Fuzzy Logic Toolbox User's Guide for Use with MATLAB*, Mathworks, Inc., 2002.